FREEPORT-McMoRan

Freeport-McMoRan Chino Mines Company
P.O. Box 10
Bayard, NM 88023

January 31, 2023

Mr. Brad Reid
New Mexico Environment Department
Ground Water Quality Bureau
PO Box 5469
Santa Fe, NM 87502

Mr. DJ Ennis
Energy, Minerals and Natural Resource Department
Mining and Minerals Division
1220 South St. Francis Drive
Santa Fe, NM 87505

Dear Mr. Reid and Mr. Ennis:

Re: Precipitation Workplan Analysis for Closure
Freeport-McMoRan Chino and Tyrone Mines

Freeport-McMoRan Chino and Tyrone Mines (Chino and Tyrone) have completed Task 2 of the Precipitation Workplan Analysis for Closure approved by NMED and MMD in a joint agency letter on September 3, 2021. As described in the Workplan, Chino and Tyrone reviewed the findings of the precipitation studies on a phone call with representatives of both NMED and MMD on January 26, 2023 and submits the enclosed report for review. As previously agreed, Chino and Tyrone with their closure design consultant, will now complete Task 3 which is to evaluate existing design criteria of closure structures against the changes projected from Task 2.

If you have any questions, please contact me at 575-912-5927 or Mr. Tom Shelley at 575-912-5773.

Sincerely,

Sherry Burt-Kested, Manager
Environmental Services

ecc: Kevin Myers, MMD
Carmen Rose, MMD

20230131-100
20230131-002

PO Box 175
Monument, CO 80132
(719) 488-4311
http://www.appliedweatherassociates.com

Climate Change Projections for the Chino/Tyrone, New Mexico Mine

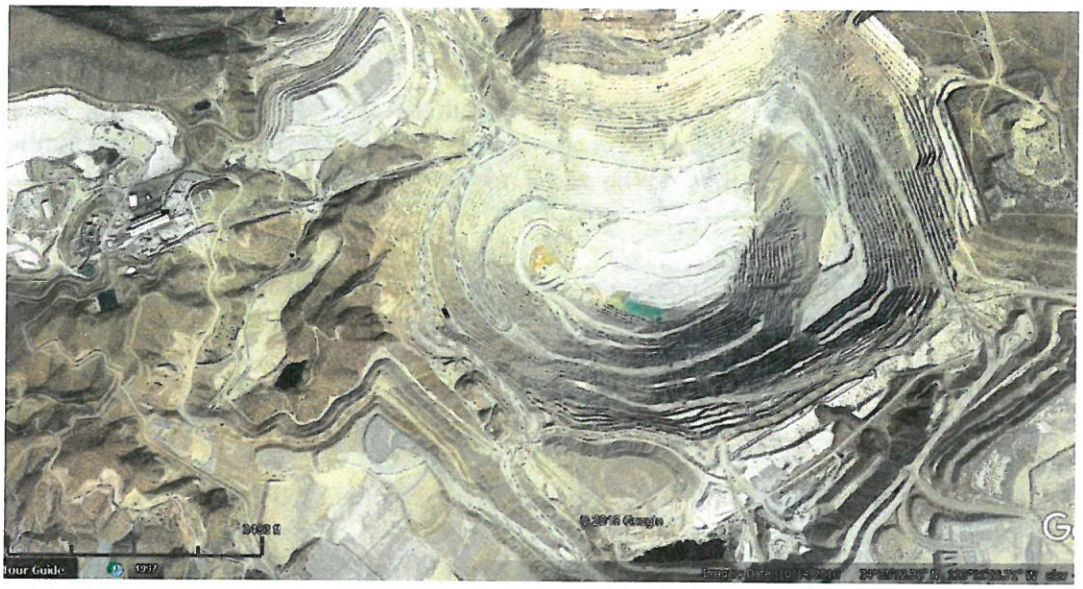

Prepared for

FREEPORT-MCMORAN

Freeport-McMoRan
333 N. Central Avenue
Phoenix, Arizona 85004

Prepared by

Applied Weather Associates, LLC
www.appliedweatherassociates.com

Doug Hultstrand, PhD, Senior Hydrometeorologist
Bill Kappel, Project Manager and Chief Meteorologist
Kristi Steinhilber, Staff Meteorologist
Marty Venticinque, Staff Meteorologist

October 2022

Notice

This report was prepared by Applied Weather Associates, LLC (AWA). The results and conclusions in this report are based upon best professional judgment using currently available data. Therefore, neither AWA nor any person acting on behalf of AWA can: (a) make any warranty, expressed or implied, regarding future use of any information or method in this report, or (b) assume any future liability regarding use of any information or method contained in this report.

DISCLAIMER

This report is an instrument of service of Applied Weather Associates, LLC (AWA). The report has been prepared for the exclusive use by Freeport-McMoRan (Client) for the specific application to the Chino/Tyrone mine, and it may not be relied upon by any other party without AWA's or the Client's written consent.

AWA has prepared this report in a manner consistent with the level of care, skill, and diligence ordinarily provided by members of the same profession for projects of similar scope at the time and place the services were rendered. AWA makes no warranty, express or implied.

Use of or reliance upon this instrument of service by the Client is subject to the following conditions:

1. The report is to be read in full, with section or parts of the report relied upon in the context of the whole report.
2. The report is based on information provided to AWA by the Client or by other parties on behalf of the Client. AWA has not verified the correctness or accuracy of such information and makes no representations regarding its correctness or accuracy. AWA shall not be responsible to the Client for the consequences of any error or omission contained in Client-supplied information.
3. AWA should be consulted regarding the interpretation or application of the findings and recommendations in the report.

Preparer Signature

Doug Hultstrand, PhD

Reviewer Signature

Bill Kappel

EXECUTIVE SUMMARY

The potential effects of climate change on meteorological characterization within the study region were assessed. Future climate change projections were determined from Regional Downscaled Climate Model (RCM) outputs specifically evaluated for the location. The Global Climate Models (GCMs), also referred to as General Circulation Models, are developed by various governmental, academic, and research agencies around the world in coordination with the Intergovernmental Panel on Climate Change (IPCC). These are utilized to set the boundary conditions and input for the RCMs. The different scenarios are described by representative concentration pathways (RCPs), a greenhouse gas concentration trajectory, often referred to as emission scenarios. As part of the IPCC analysis, four pathways were applied for climate modeling: RCP 2.6, RCP 4.5, RCP 6.0, and RCP 8.5 (IPCC, 2017). The various pathways considered different climate futures, depending on the volume of greenhouse gases (GHG) emitted in the years to come. Climate change studies that evaluate future temperature and precipitation projections utilize the middle of the road emission scenario (RCP 4.5) and the most extreme emission scenario (RCP 8.5). These provide a bracket of the projections that utilize the most likely outcome (RCP 4.5) and the most unlikely outcome (RCP 8.5).

For this study, climate model projections gridded outputs were investigated for the three scenarios: i) historic, ii) RCP 4.5, and iii) RCP 8.5. The historical period is based on daily data from 1950 through 2005, and the RCP periods are based on daily data from 2006 through 2100. The North American CORDEX gridded daily time-series data, which cover the study area, were extracted, aggregated, and applied for the climate change analysis as part of the 2022 regional work by Deloitte. The climate model projections were used to analyze precipitation trends, precipitation frequency, and maximum precipitation for the 1-day, 3-day, and annual durations for the area covering the study region. Results of the analysis are presented in Table E.1. For hydrologic simulation and sensitivity, the ensemble median RCP 4.5 climate change adjustments and uncertainty values for temperature and precipitation are recommended. The results are based on an evaluation of rate of change from the current period through 2100. These values can be applied to a given period (i.e., 2050) by linearly adjusting the climate change factors.

Table E.1: Climate Change Projections from current climate (1950-2014) through 2100.

	RCP45				RCP85			
	Mean	**Median**	**Min**	**Max**	**Mean**	**Median**	**Min**	**Max**
Temperature 1-Day; C	**1.6**	**2.1**	-1.3	2.9	**5.3**	**5.0**	4.5	6.4
Temperature 1-Day Monsoon PF; C	**1.6**	**2.1**	-1.3	2.9	**5.3**	**5.0**	4.5	6.4
Temperature 1-Day Winter PF; C	**1.8**	**2.4**	-1.4	3.0	**5.6**	**5.8**	5.3	5.9
+Precipitation 1-Day PF; %	**16**	**22**	-31	49	**35**	**40**	-18	69
Precipitation 1-Day Monsoon PF; %	**15**	**14**	-20	48	**28**	**27**	-32	64
Precipitation 1-Day Winter PF; %	**-1**	**-7**	-29	24	**12**	**12**	-7	41
+Precipitation 3-Day PF; %	**4**	**5**	-13	15	**14**	**24**	-8	31
Precipitation 3-Day Monsoon PF; %	**5**	**3**	-9	15	**11**	**23**	-18	28
Precipitation 3-Day Winter PF; %	**9**	**0**	-26	79	**6**	**7**	-17	19
Precipitation Annual PF; %	**2**	**-1**	-15	13	**2**	**-2**	-21	28
PMP 1-Day, %	**No Change**				**Potential Increase**			
PMP 3-Day; %	**No Change**				**No Change**			

TABLE OF CONTENTS

LIST OF FIGURES

LIST OF TABLES

LIST OF APPENDICES

Acronyms and Abbreviations

AEP	Annual Exceedance Probability
AMS	Annual Maximum Series
ARF	Areal Reduction Factor
ARI	Average Recurrence Interval
AWA	Applied Weather Associates
CDF	Cumulative Distribution Function
GCM	Global Climate Model or General Circulation Model
GEV	Generalized Extreme Value distribution
GHCN	Global Historical Climatology Network
GHG	Green House Gas
GLO	Generalized Extreme Value distribution
GNO	Generalized Normal distribution
GPA	Generalized Pareto distribution
IPCC	Intergovernmental Panel on Climate Change
L-Cv	L-moment coefficient of L-variation
L-Kurtosis	L-moment ratio of kurtosis
L-Skewness	L-moment ratio of skewness
MAM	Mean Annual Maximum
MAP	Mean Annual Precipitation
NCDC	National Climate Data Center
NCEI	National Centers for Environmental Information
NOAA	National Oceanic and Atmospheric Administration
PE3	Pearson Type III distribution
PF	Precipitation-Frequency
POR	Period of Record
Ppt	Precipitation
Ppt_{adj}	Maximized Precipitation
Ppt_{max}	Largest Thirty Precipitation Events
Ppt_{pmp}	Maximum of Largest Thirty Maximized Precipitation Events
PRISM	Parameter-elevation Regressions on Independent Slopes Model
Press	Surface Pressure
QC	Quality Control
RCP	Representative Concentration Pathway
RGC	Regional Growth Curve
RH	Relative Humidity
SH	Specific Humidity
SP	Shared Socioeconomic Pathways
SSP	Shared Socioeconomic Pathways
Ta	Air Temperature
Td	Dew Point Temperature

1.0 INTRODUCTION

Applied Weather Associates (AWA) examined climate model projections to analyze precipitation trends, precipitation frequency, and maximum precipitation for the 1-day, 3-day, and annual durations for the region covering the Chino/Tyrone Mine, New Mexico study region (Figure 1). Three different investigations were completed each of which provided a different look at the climate change projections. The first method investigated station and climate projection trends using trend analysis methods based on Mann (Mann, 1945) and Hipel and McLeod (2005) utilizing the R-statistical software packages 'Kendall' developed by McLeod (2015). The second method was precipitation frequency analysis based on L-moments methods described in Hosking and Wallis (1997) and utilized the R-statistical software packages 'lmom' and 'lmomRFA' developed by Hosking (Hosking 2015a, and Hosking 2015b). The third method identified the largest precipitation events from the daily climate projections, derived monthly dew point temperature climatologies from the climate model projections and maximized the storm events through storm maximization methods (Rousseau et al., 2014; Kappel et al., 2018; Kappel et al., 2020). In addition, climate change for mean monthly and annual climatologies were derived for precipitation and temperature.

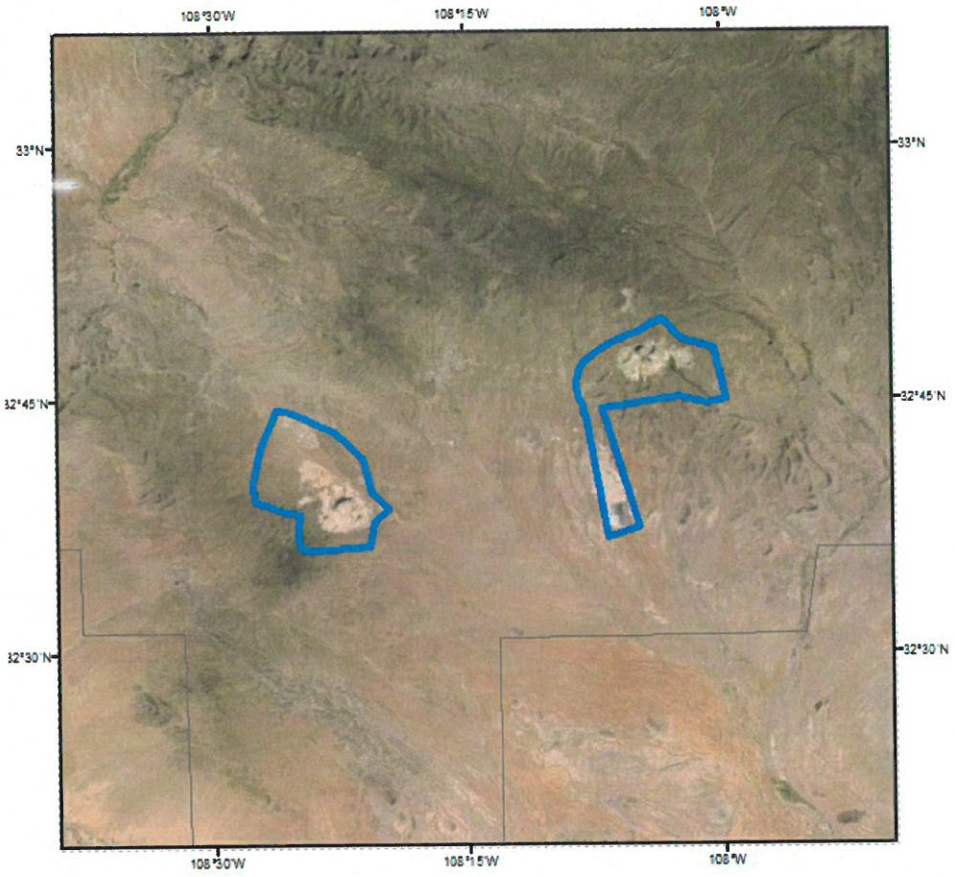

Figure 1: Location of the Chino/Tyrone study region.

2.0 CLIMATE CHANGE PROJECTION BACKGROUND

Climate is changing, always has been changing, and always will change as long as the energy received from the across the Earth's surface and atmosphere is not distributed evenly. Accounting for future changes in climate is important to reduce risk and ensure infrastructure is designed to safely manage potential future changes. Unfortunately, quantification of the amount and rate of change at any given location for any specific meteorological parameter is not explicitly quantifiable and instead has to be modeled based on our incomplete understanding of the Earth's climate system and future atmospheric composition. Therefore, model projections that utilize our current understanding of the Earth climate system are developed. The climate projections are based on our best quantification of physical understanding of numerous atmospheric parameters and how those affect weather and climate through time and space. However, because our quantification of these parameters are incomplete (and at times inaccurate) and because we currently have a limited understanding of the various interactions and feedbacks, the climate projections represent possible outcomes. None of which can be considered truth, but instead should be treated as "what if" scenarios representing possible outcomes.

To better address these significant limitations, numerous iterations and sensitivity analyses for various atmospheric parameters are performed so that a suite of ensembles are produced to represent a wide range of potential outcomes. From this output, inferences can be made, with more confidence given when ensemble outcomes converge on a common projection. Another layer of uncertainty within the climate change projection process relates to the assumption applied for future emissions scenarios and how those may affect the climate system. Future emissions scenarios have two major areas of uncertainty. First, our assumption that any given emission scenario will occur following a specific path through time is unknown as there are many internal and external factors that can influence the amount of emissions produced through time. Second, our understanding and quantification of how the Earth's climate will respond to any given greenhouse gas emission is limited. Both uncertainties introduce errors into the climate projections. Finally, the GCMs are computationally intensive and are therefore run at low resolution both in time and space. For regions like the Chino/Tyrone basin, the resolution of the GCMs is inadequate to capture the spatial variations. To overcome this, projections from GCMs are downscaled using a statistical process into regional downscaled model projections. RCMs are downscaled and are what were utilized for this climate change analysis. Given all the limitations and uncertainties noted above, it is still useful to evaluate RCMs to understand the range of potential outcomes that could occur through time over the basin.

2.1 Global Climate Change Models

GCMs produce realizations of the Earth's climate on a generally coarse scale of around 1000km by 1000km. Because the scale is so coarse, a single GCM grid may cover vastly differing landscape (from very mountainous to flat coastal plains for example) with greatly varying potential for floods, droughts, or other extreme events.

2.2 Regional Downscaled Climate Change Models

RCMs and Empirical Statistical Downscaling applied over limited areas cover a much finer resolution. These are therefore able to capture the spatial and temporal variations related to a site-specific region, such as the Chino/Tyrone study region. The downscaling methods are driven by

GCMs, where the RCM is nested within the overall GCM and utilizes the GCM to set the initial boundary conditions. These are then downscaled using either the statistical methodology or the RCM based on a meteorological model interface. The RCM process can provide projections of future climate conditions on a much smaller scale (e.g., < 50km by 50km) supporting more detailed site-specific information allowing for adaptation assessment and planning. An example of different climate model resolutions across the Chino/Tyrone region are shown in Figure 2.

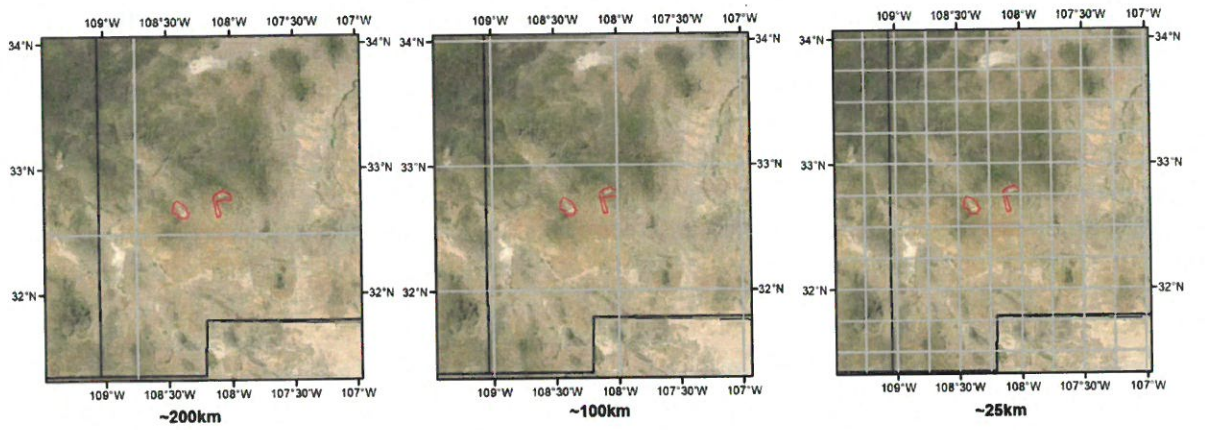

Figure 2: Example of different global and regional climate model resolutions across the Chino/Tyrone region.

3.0 CLIMATE CHANGE PROJECTION ANALYSIS METHODS

The Intergovernmental Panel on Climate Change (IPCC) fifth assessment report (AR5) contains representative concentration pathway (RCP)s, a greenhouse gas concentration trajectory, often referred to as emission scenarios. As part of this analysis, four pathways were applied for climate modeling and research for the IPCC AR5 (IPCC, 2017). The pathways describe different climate futures, all of which are considered possible depending on the volume of greenhouse gases (GHG) emitted in the years to come (Figure 3). The RCPs investigated; RCP 2.6, RCP 4.5, RCP 6.0, and RCP 8.5; are labeled after a possible range of radiative forcing values in the year 2100 (IPCC, 2017; IPCC, 2021).

Regional downscaled climate model projections from the Coupled Model Intercomparison Project Phase 5 (CMIP5) outputs based on IPCC AR5 projections were used in this study and extracted from the Coordinated Regional Climate Downscaling Experiment (CORDEX). The uncertainty in climate projections is typically represented by the range of climate futures indicated by the CMIP5 ensemble of projections (McSweeney and Jones, 2016). The purpose of this output is to provide a set of global, high resolution, bias-corrected climate change projections that can be used to evaluate climate change impacts on processes that are sensitive to finer-scale climate gradients and the effects of local topography on climate conditions. For this study, five climate model projections were investigated for the three scenarios: i) historic, ii) RCP 4.5, and iii) RCP 8.5. The historical period is based on daily data from 1950 through 2005, and the RCP periods are based on daily data from 2006 through 2100.

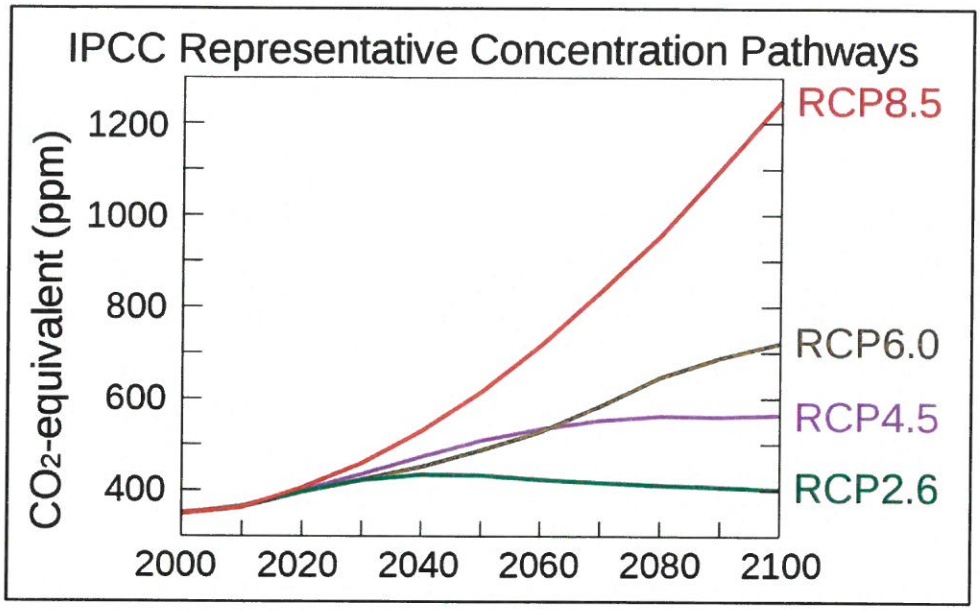

Figure 3: Representative concentration pathway (RCP) trajectories. Reproduced from IPCC (2017).

The key climate model parameters used in this analysis were precipitation (Ppt), air temperature (Ta), and dew point temperature (Td). The parameters of relative humidity (RH), specific humidity (SH), and surface pressure (Press) were used to derive the estimates of dew point (Td). The North American CORDEX interface consists of thirty models (five GCMs driving five RCMs), of these thirty models, five models had the parameters and projections needed for the climate change analysis (Figure 4). The North American CORDEX outputs were extracted, quality controlled, and formatted as part of the 2022 regional work by Deloitte. The HadGEM2-ES GCM model was not used for time-series analysis because it has a 360-day calendar where each month is 30 days in length and only has data for RCP 8.5 up to 30-Nov-2099. An example of the modeled daily climate projection parameters of Ppt, Ta, and Td are shown in Figure 5 and the number of grids and weighting applied covering the study region are shown in Figure 6. The climate projections historical period is based on daily data from 1950 through 2005, and the future periods are based on daily data from 2006 through 2100.

nulation/Model	1	2	3	4	5
Driving Global Climate Model (GCM)	CCCma-CanESM2	CCCma-CanESM2	CNRM-CERFACS-CNRM-CM5	MPI-M-MPI-ESM-LR	NOAA-GFDL-GFDL-ESM2M
Climate Model (RCM)	CanRCM4	CRCM5	CRCM5	CRCM5	CRCM5
ly Precipitation	✓	✓	✓	✓	✓
Daily Average Surface Temperature	✓	✓	✓	✓	✓
Daily Maximum Surface Temperature	✓	✓	✓	✓	✓
Surface Humidity	✓	✓	✓	✓	✓
Surface Pressure	✓	✓	✓	✓	✓
y Snow Amount[4]	✗	✓	✗	✓	✗
c Simulation Years	1951-2005	1951-2005	1951-2005	1951-2005	1951-2005
RCP2.6	✗	✗	✗	✗	✗
RCP4.5	2006-2100	2006-2100	2006-2100	2006-2100	2006-2100
RCP8.5	2006-2100	2006-2100	2006-2100	2006-2100	2006-2100
Resolution	NAM-22	NAM-22	NAM-22	NAM-22	NAM-22

Figure 4: Subset of CMIP5 models and the parameters and projections used for the climate change analysis

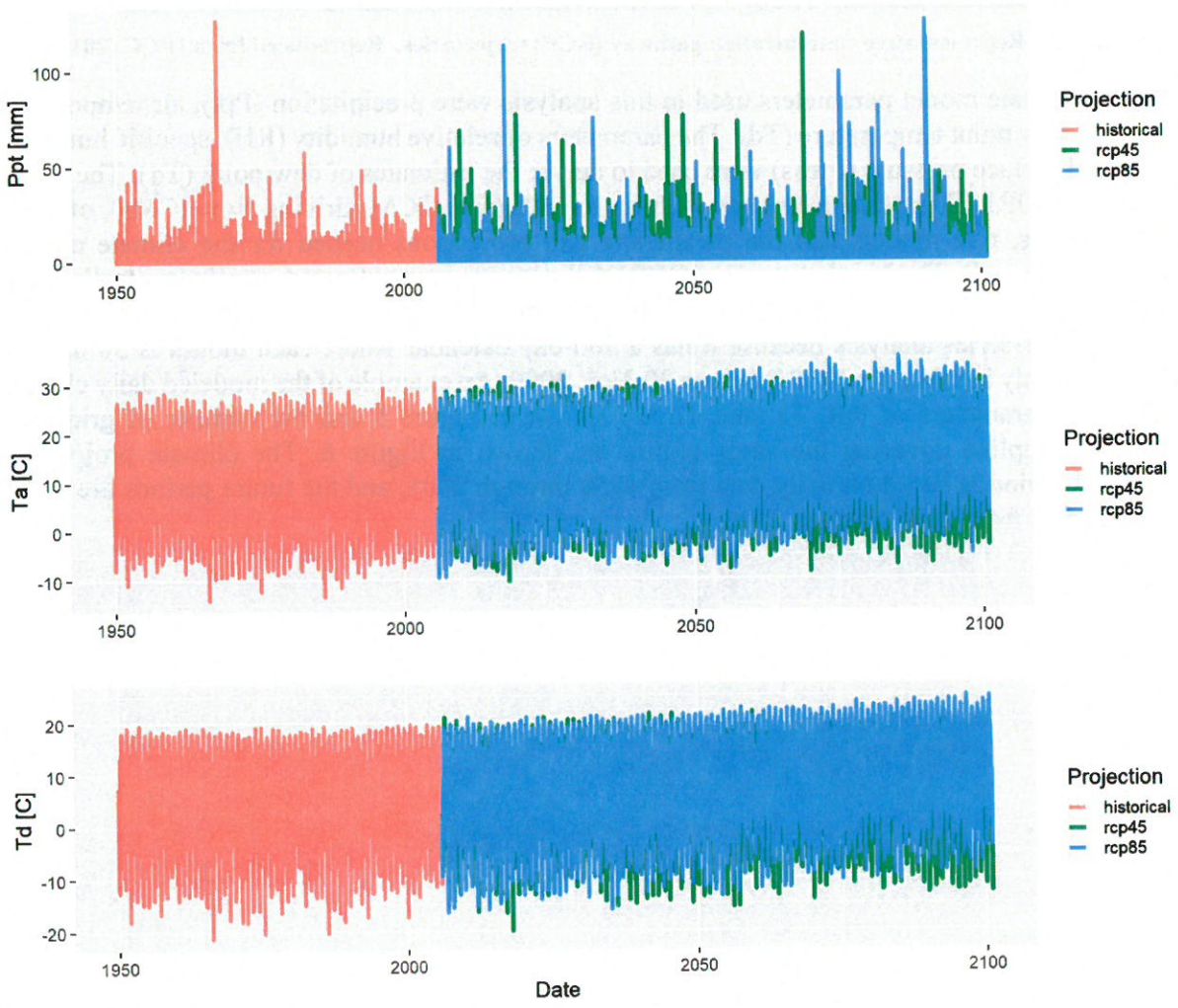

Figure 5: Climate projection parameters of Ppt, Ta, and Td from Model 1 (NAM22 CanRCM4 CanESM2)

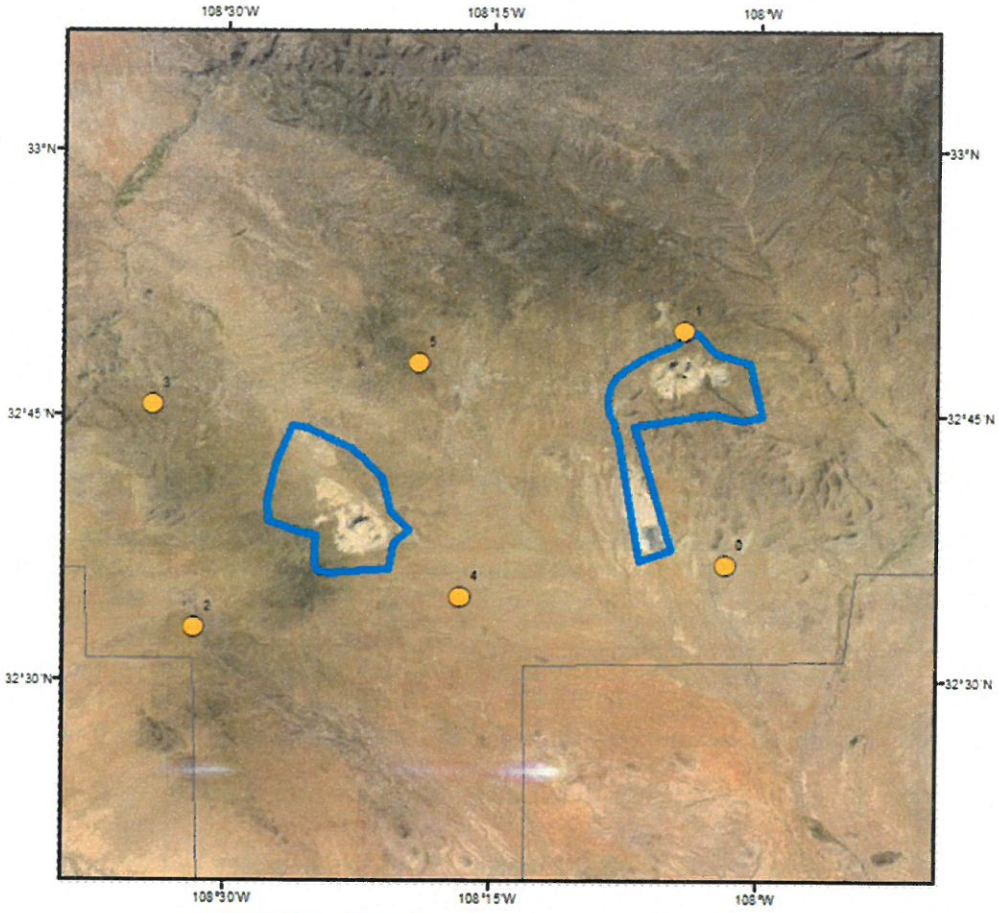

Point	Latitude	Longitude
0	32.61	-108.03
1	32.83	-108.07
2	32.55	-108.53
3	32.76	-108.57
4	32.58	-108.28
5	32.8	-108.32

Figure 6: CMIP5 climate model grids and weights used for climate change analysis (modified from Deloitte regional work 2022). The blue triangle represents the mine locations, and the colored circles represent the CORDEX grid centers and associated weighting.

3.1 Trend Analysis

Mann-Kendall trend analysis (Mann, 1945; Hipel and McLeod, 2005) was performed on the Chino/Tyrone climate station located near the mine site for 1-day, 3-day, and annual durations. Results of these station-based trend analysis are shown in Table 1. The climate station trend results were used to assess the historic model projections.

Table 1: Climate stations used for trend analysis. Trend analyses are tested at the 0.05 significant level.

	Precipitation			Temperature
	1-day	3-day	Annual	1-day
Redrock	no trend	no trend	no trend	no trend
Fort Bayard	no trend	no trend	no trend	no trend

In addition, Mann-Kendall trend analysis (Mann, 1945; Hipel and McLeod, 2005) was performed on five climate model projections using the three scenarios (historic, RCP 4.5, RCP 8.5) for durations of 1-day, 3-day, and annual. Figure 7 shows and example of the results for Model 1 1-day trend analysis for the historic, RCP 4.5, and RCP 8.5 projections. Results for all the climate model projection trend analyses are summarized in Table 2. Detailed results are included in Appendix B.

Table 2: Summary of climate projection trend analysis results. Trend analyses are tested at the 0.05 significant level.

	Precipitation			Temperature
	1-day	3-day	Annual	1-day
Historic	5 – no trend 0 – increase 0 – decrease	5 – no trend 0 – increase 0 – decrease	5 – no trend 0 – increase 0 – decrease	4 – no trend 1 – increase 0 – decrease
RCP 4.5	5 – no trend 0 – increase 0 – decrease	5 – no trend 0 – increase 0 – decrease	4 – no trend 0 – increase 1 – decrease	0 – no trend 5 – increase 0 – decrease
RCP 8.5	5 – no trend 0 – increase 0 – decrease	5 – no trend 0 – increase 0 – decrease	2 – no trend 1 – increase 2 – decrease	0 – no trend 5 – increase 0 – decrease

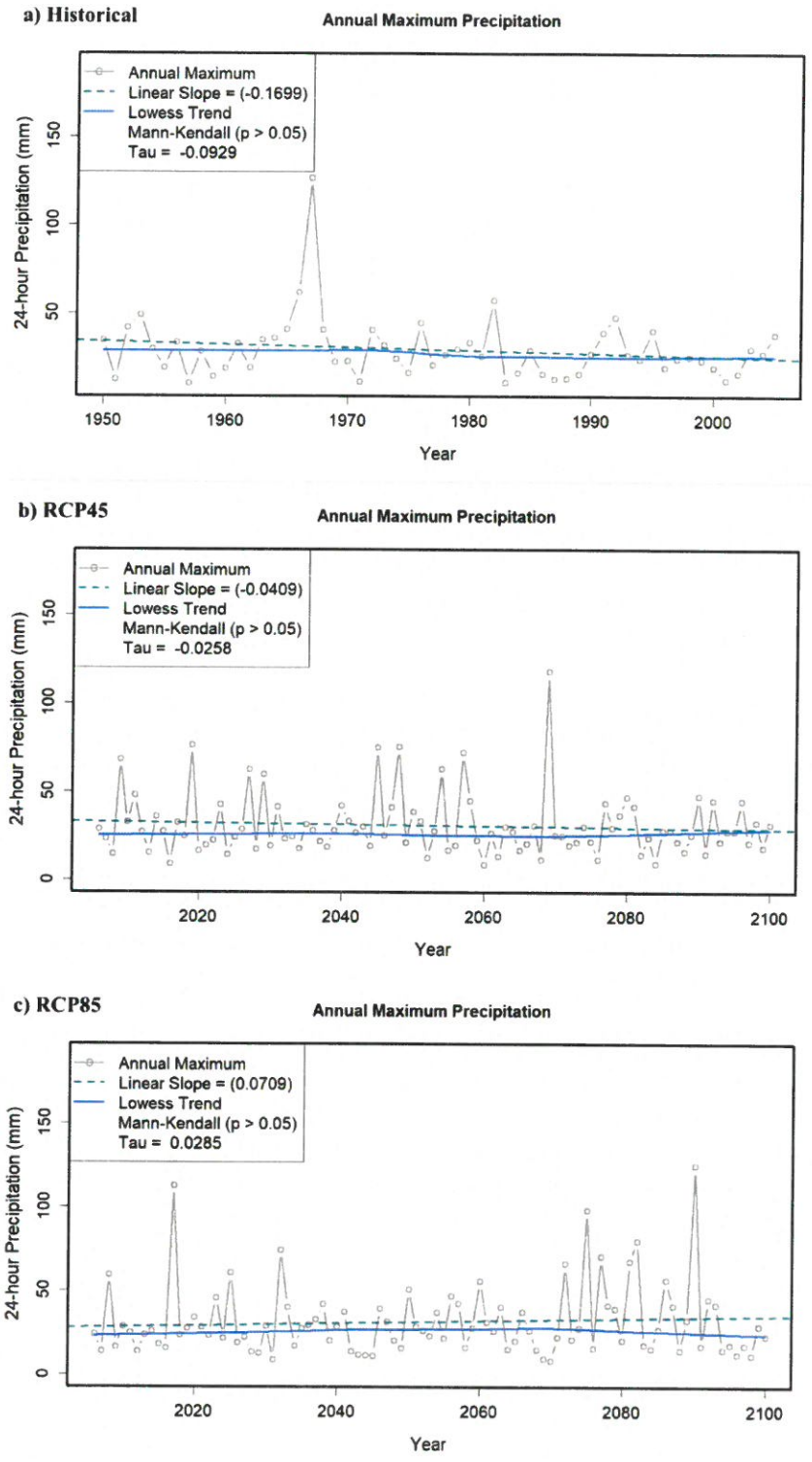

Figure 7: Example results for 1-day trend analysis for climate projection from Model 1: a) no trend for historical period, b) no trend for RCP 4.5 scenario, and c) no trend for RCP 8.5 scenario. Blue line is Lowess trend line, dashed line is a linear trend, and Mann-Kendall p-value and Tau statistics shown in legend.

3.2 Precipitation Frequency Analysis

The precipitation frequency analysis method utilized L-moment statistics instead of product moment statistics, which decrease the uncertainty of rainfall frequency estimates for more rare events and dampens the influence of outlier precipitation amounts from extreme storms (Hosking and Wallis, 1997). Methods to account for non-stationarity in projections were not addressed, the projections were applied assuming stationarity. For the precipitation frequency analysis, AWA utilized the daily climate model projections to perform frequency analysis on the 1-day, 3-day, and annual durations.

AWA evaluates the climate change projections for the entire period available, for CMIP5 that ranges from 2005 through 2100. The changes through time reflect the entire period. However, other evaluation periods can be considered and may change the rate of change through time. For example, one may evaluate the projections through the year 2050 and then do a separate analysis for the years 2050-2100. This may result in slightly different outcomes depending on the climate change projections changes through time. For example, some climate change models may show minimal changes for the period 2005 through 2050, then an increasing change from 2051 through 2100. Regardless of the process utilized to evaluate the climate change projections and the increments evaluated, it is recommended that each iteration of the IPCC climate change outputs be evaluated against the previous work to check trends and changes.

AWA identified, extracted, and quality controlled maximum precipitation projections for the five models and three projection scenarios. The Annual Maximum Series (AMS) were then subjected to the frequency analysis methods (Hosking and Wallis, 1997). L-moment statistics were computed for annual maximum data for each projection and duration. Goodness of fit measures were evaluated for five candidate distributions: generalized logistic (GLO), generalized extreme value (GEV), generalized normal (GNO), Pearson type III (PE3), and generalized Pareto (GPA). An L-Moment Ratio Diagram was prepared based on L-Skewness and L-Kurtosis pairs for each duration (Figure 8). The weighted-average L-Skewness and L-Kurtosis pairing were found to be near the GEV distribution for all projections.

The GEV distribution was selected because: i) This is the most common distribution used for precipitation frequency studies (e.g., NOAA Atlas 14, Perica, 2015) ii) the GEV was identified on both the 1-day, 5-day, 90-day, and Annual goodness-of-fit measures, and iii) using the same distribution ensures a more direct comparison to more rare values of the frequency curve. The GEV is a general mathematical form that incorporates Gumbel's Extreme Value (EV) type I, II and III distributions for maxima. The parameters of the GEV distribution are the ξ (location), α (scale), and k (shape). The Gumbel EV type I distribution is obtained when $k = 0$. For $k > 0$, the distribution has a finite upper bound at $\xi + \alpha / k$ and corresponds to the EV type III distribution for maxima that are bounded above. For $k < 0$, this corresponds to the Gumbel EV type II distribution.

The uncertainty analysis for deriving the frequency curve and uncertainty bounds were conducted as follows. The frequency distributions were randomly permuted, and data were simulated from the selected frequency distribution. The procedure is described in Hosking and Wallis (1997) and Hosking (2015b), except that the permutation of frequency distributions is a later modification, intended to give more realistic sets of simulated data (Hosking, 2015b). From each permutation the sample mean values and estimates of the quantiles of the regional growth curve, for non-

exceedance probabilities are saved. From the simulated values, for each quantile specified the relative root mean square error (relative RMSE) is computed as in Hosking and Wallis (1997). The error bounds are sample quantiles of the ratio of the estimated regional growth curve to the true at-site growth curve of the ratio of the estimated to the true quantiles at individual sites (Hosking, 2015b).

In order to separate Summer/Monsoon season and Winter season precipitation events that are controlling of the yearly precipitation regime in the Chino/Tyrone region, the 1-day and 3-day annual maximum were also extracted for the Summer/Monsoon season (May - October) and for the Winter season (November – April). The summer and winter AMS data were used to perform L-moment frequency analysis methods as described above. Comparisons of percent change were made among model projections for 10-year through 1,000-year recurrence intervals, beyond this the uncertainty in probability distributions estimates is large. Figure 8 shows and example of the results for Model 1 1-day precipitation frequency analysis for All season (mixed storm distribution), Summer/Monsoon season, and Winter season for the historic, RCP 4.5, and RCP 8.5 projections. Full results of frequency analysis are included in Appendix B.

***** 1-Day Precipitation**

	10yr	50yr	100yr	500yr	1000yr	Pct Change					Average
Historical	49.1	76.2	89.9	128.1	147.8	-	-	-	-	-	
RCP45	51.3	83.3	100.6	152.2	180.5	5%	9%	12%	19%	22%	**13%**
RCP85	55.5	97.8	122.2	199.9	245.2	13%	28%	36%	56%	66%	**40%**

***** 1-Day Monsoon**

	10yr	50yr	100yr	500yr	1000yr	Pct Change					Average
Historical	40.5	76.6	98.9	176.2	224.7	-	-	-	-	-	
RCP45	45.3	84.2	107.6	185.3	232.5	12%	10%	9%	5%	3%	**8%**
RCP85	42.6	89.9	122.4	247.3	333.7	5%	17%	24%	40%	49%	**27%**

***** 1-Day Winter**

	10yr	50yr	100yr	500yr	1000yr	Pct Change					Average
Historical	36.8	52.1	59.0	75.6	83.2	-	-	-	-	-	
RCP45	36.5	49.9	55.4	68.0	73.3	-1%	-4%	-6%	-10%	-12%	**-7%**
RCP85	41.8	67.8	81.3	119.5	139.5	14%	30%	38%	58%	68%	**41%**

Figure 8: Example results for 1-day precipitation frequency analysis for climate projection from Model 1.

3.3 Maximum Precipitation Analysis

Dew Point climatologies based on the climate model projections were developed for the 24-hour duration for use in the in-place storm maximization. Dew point information is utilized to maximize observed precipitation events during PMP calculations as a way to quantify the amount of moisture available to a given storm event versus how more moisture could have been available to that storm had higher dew point values (and hence moisture) been available. Therefore, quantifying the change in dew point values from future climate change projections is important. The assumption

is that if more moisture is available in the future, more precipitation could occur. However, the response of the atmosphere between increasing moisture capacity and resulting precipitation is not a linear relationship. Instead, there are numerous positive and negative feedbacks, some that are quantified and some that are not. This is why it is not appropriate to simply apply the Clausius Clapeyron equation, which produces a 7% increase in moisture holding capacity of the air mass for every 1° C increase in temperature, to determine future precipitation estimates based on a given temperature increase. Instead, AWA calculated the ratio of dew point maximizations from climate change projections as a way to compare against the ratio utilized in the current climate data.

This method follows the in-place storm maximization process used in PMP studies completed by AWA, the National Weather Service, and described in the World Meteorological Organization Manual for PMP (2009) (US Weather Bureau, 1951; Kappel et al., 2014-2022). For each model projection, AWA developed monthly 100-yr dewpoint climatologies following the process described in previous AWA PMP studies (e.g., Kappel et al., 2014; Kappel et al., 2018; Kappel et al., 2021).

3.3.1 Dew Point Climatology

A script was written to extract each climate projections' monthly maximum dew point temperatures for the 24-hour duration for each year, providing the AMS. This was done to calculate the maximum precipitation (Ppt_{adj}) following the in-place maximation process. The AMS for each month for each projection served as input to an R-statistical script that calculated L-moment statistics (Section 3.2). Using the generalized-extreme-value (GEV) distribution, the 20-year, 50-year, and 100-year return frequency dew point temperature values were calculated for each month for each projection (Figure 9). The extracted dew point data were adjusted to the 15th of each month.

The results indicate small monthly variability in the 100-year dew point climatologies. Most months are within +/- 2-3° C, and the differences between model projections (historic, RCP 4.5, and RCP 8.5) seem to be scaled by 2-3° C. An example comparison of the monthly 100-year dew point climatologies for Model 1 are shown in Figure 10. Note, the historic and two future 100-year dew point climatologies projected by climate Model 1 are lower than the AWA station derived 100-year dew point climatology used for PMP studies, climate Model 1 shows negligible change in the summer (May – October) dew point climatologies with an increase in moisture during the early winter to spring period.

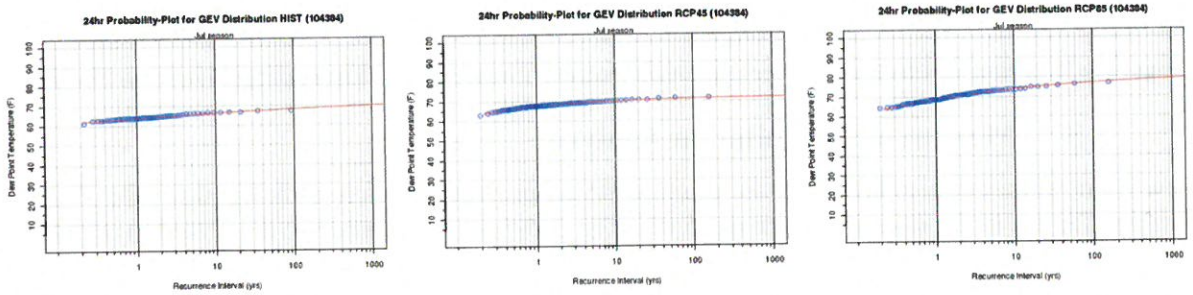

Figure 9: Example of July 24-hour dew point frequency analysis results for Model 1 projections (historical, RCP 4.5, RCP 8.5).

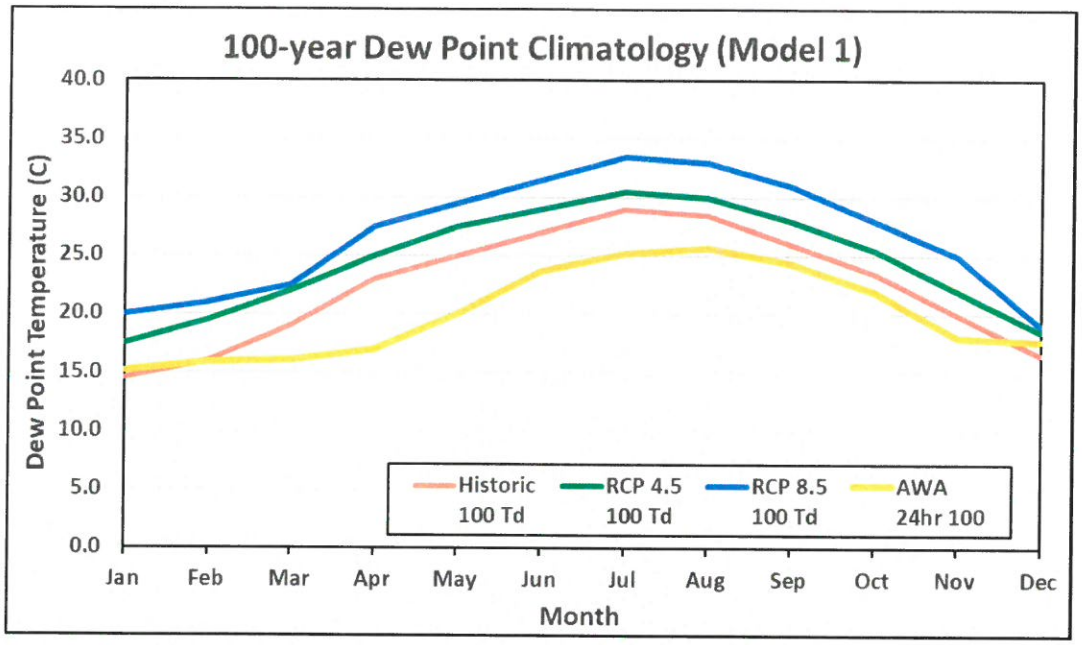

Figure 10: Results of Model 1 dew point 100-year climatology for 24-hour duration by model projections. The AWA dew point profile is based on AWA's updated dew point climatology (Kappel et al., 2018), this illustrates a cooler/less moisture atmosphere than all three of Model 1 dew point projections.

3.3.2 Precipitation Maximization

A script was written to extract each climate projections' thirty largest 24-hour and 72-hour precipitation estimates (Ppt_{max}). Adjustments used to maximize Ppt_{max} precipitation (Ppt_{adj}) for each precipitation event were estimated following the same in-place maximization process as applied during the PMP calculation process. This is completed by multiplying the climate model projection actual precipitation (Ppt_{max}) by a maximization ratio r:

$$Ppt_{adj} = Ppt_{max} * r$$

where r is defined as the ratio of the maximized precipitable water (using the 100-year dew point climatology either from observation data or climate change projections and assuming a pseudo-adiabatic lapse rate through the atmosphere from the surface to 300mb) to the actual event's precipitable water (storm events observed dew point) following methods used in storm-based PMP studies (e.g., Hansen et al., 1988; Kappel et al., 2014; Kappel et al., 2018). The resulting maximized climate change projected precipitation event is analogous to PMP (Ppt_{pmp}) in that is corresponds to the greatest maximized precipitation event (max(Ppt_{adj})) over the climate change projection period. The largest thirty 1-day events (Ppt_{max}) and the maximized thirty events (Ppt_{adj}) are shown for Model 1 projections in Figure 11. The largest thirty 3-day events (Ppt_{max}) and the maximized thirty events (Ppt_{adj}) are shown for Model 1 projections in Figure 12. Comparisons of percent change between Ppt_{pmp} and the Ppt_{max} and Ppt_{adj} were made among model projections (historical, RCP 4.5, RCP 8.5) and shown in Table 3 for 1-day and Table 4 for 3-day. This provided a range of expected change in the maximization parameters associated with PMP type events from the climate change projections.

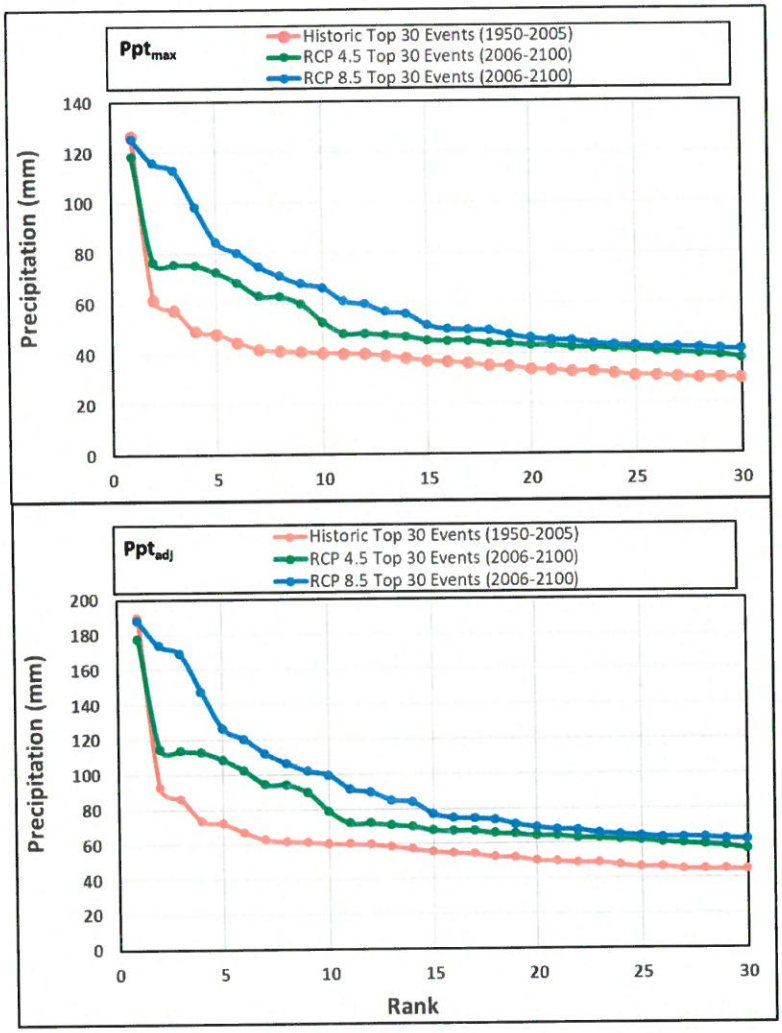

Figure 11: Results of the 1-day largest thirty events (Ppt_{max}) and the maximized thirty (Ppt_{adj}) events for Model 1.

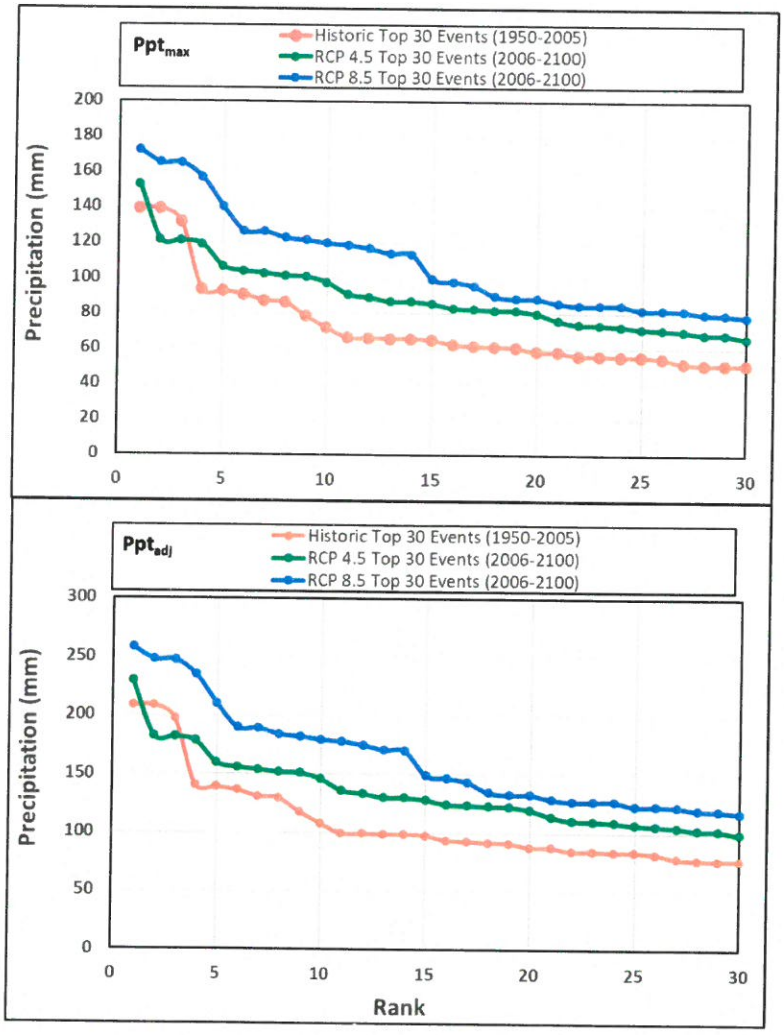

Figure 12: Results of the 3-day largest thirty events (Ppt_{max}) and the maximized thirty (Ppt_{adj}) events for Model 1.

Table 3: Comparisons of 1-day percent change between (Ppt_{pmp}) and the (Ppt_{max}) and (Ppt_{adj}) made among model projections

NAM22 CanRCM4 CanESM2

Ppt_{max}	(mm)	Pct Change	Ppt_{adj}	(mm)	rank	Pct Change
Historical	126.5	-	Historical	189.7	1	-
RCP45	118.4	-6%	RCP45	177.5	1	-6%
RCP85	125.2	-1%	RCP85	187.8	1	-1%

NAM22 CRCM5 CanESM2

Ppt_{max}	(mm)	Pct Change	Ppt_{adj}	(mm)	rank	Pct Change
Historical	81.3	-	Historical	121.9	1	-
RCP45	55.1	-32%	RCP45	82.7	1	-32%
RCP85	63.5	-22%	RCP85	95.3	1	-22%

NAM22 CRCM5 CERFACS CNRM

Ppt_{max}	(mm)	Pct Change	Ppt_{adj}	(mm)	rank	Pct Change
Historical	67.6	-	Historical	101.3	1	-
RCP45	73.7	9%	RCP45	110.5	1	9%
RCP85	106.2	57%	RCP85	159.3	1	57%

NAM22 CRCM5 MPT MPI ESM LR

Ppt_{max}	(mm)	Pct Change	Ppt_{adj}	(mm)	rank	Pct Change
Historical	74.4	-	Historical	111.6	1	-
RCP45	125.5	69%	RCP45	188.2	1	69%
RCP85	159.8	115%	RCP85	239.6	1	115%

NAM22 CRCM5 NOAA GFDL ESM2

Ppt_{max}	(mm)	Pct Change	Ppt_{adj}	(mm)	rank	Pct Change
Historical	89.9	-	Historical	134.9	1	-
RCP45	109.2	21%	RCP45	163.8	1	21%
RCP85	120.4	34%	RCP85	180.6	1	34%

Table 4: Comparisons of 3-day percent change between (Ppt_{pmp}) and the (Ppt_{max}) and (Ppt_{adj}) made among model projections

NAM22 CanRCM4 CanESM2						
Ppt_{max}	(mm)	Pct Change	Ppt_{adj}	(mm)	rank	Pct Change
Historical	139.2	-	Historical	208.8	1	-
RCP45	152.9	10%	RCP45	229.4	1	10%
RCP85	172.2	24%	RCP85	258.3	1	24%

NAM22 CRCM5 CanESM2						
Ppt_{max}	(mm)	Pct Change	Ppt_{adj}	(mm)	rank	Pct Change
Historical	94.7	-	Historical	142.1	1	-
RCP45	93.5	-1%	RCP45	140.2	1	-1%
RCP85	85.1	-10%	RCP85	127.6	1	-10%

NAM22 CRCM5 CERFACS CNRM						
Ppt_{max}	(mm)	Pct Change	Ppt_{adj}	(mm)	rank	Pct Change
Historical	101.6	-	Historical	152.4	1	-
RCP45	122.7	21%	RCP45	184.0	1	21%
RCP85	137.9	36%	RCP85	206.9	1	36%

NAM22 CRCM5 MPT MPI ESM LR						
Ppt_{max}	(mm)	Pct Change	Ppt_{adj}	(mm)	rank	Pct Change
Historical	164.6	-	Historical	246.9	1	-
RCP45	180.1	9%	RCP45	270.1	1	9%
RCP85	238.3	45%	RCP85	357.4	1	45%

NAM22 CRCM5 NOAA GFDL ESM2						
Ppt_{max}	(mm)	Pct Change	Ppt_{adj}	(mm)	rank	Pct Change
Historical	157.7	-	Historical	236.6	1	-
RCP45	200.2	27%	RCP45	300.2	1	27%
RCP85	186.4	18%	RCP85	279.7	1	18%

3.4 Uncertainty

Measurement, modeling, and simulation of many meteorologic components can be highly uncertain, the main reason being the fundamental dynamics of many processes cannot be measured and modeled accurately (Kampf et al., 2020). Most meteorologic processes are not observed in detail, consequently accurate mathematical representation of the variables spatial and temporal processes, model initial boundary layer conditions, and physical processes, cannot be represented accurately. Mantovan and Tondini (2006) have identified sources of water balance uncertainties as: (i) data uncertainty, (ii) model parameter uncertainty, (iii) model structure uncertainty, and (iv) natural uncertainty.

3.4.1 Data Uncertainty

The performance of models is mainly affected by data uncertainty. This uncertainty arises from errors in the observed data, particularly data used for model calibration. The errors may be linked to the quality of the data which depends on the type and conditions of measuring instruments as well as data handling and processing. Precipitation and streamflow are usually the major sources of input and output data that are used to calibrate and evaluate model uncertainty with the spatial and temporal precipitation uncertainty being large.

3.4.2 Model Parameter Uncertainty

Model parameter uncertainty is also known as model specification uncertainty. This relates to the inability to converge to a single best parameter set using available data, which leads to parameter identifiability problems (Beven, 2001; Wagener et al., 2004). The parameters are optimized so that the model results are as good as possible (Beven, 2001; Scharffenberg et al., 2018). Uncertainty then depends on how parameters are optimized (peak flow, volume, residuals) and results are applied (Scharffenberg et al., 2018; Pokorny et al., 2021).

3.4.3 Model Structure Uncertainty

Model structure uncertainty is introduced through simplifications and/or inadequacies in the representation of physical processes in a given model. It also originates from inappropriate assumptions within the modelling procedure, inappropriate mathematical description of these processes (Beven, 2001), and the scale at which processes are represented in the model (Heuvelink, 1998; Blöschl, 1999; Koren et al., 1999). However, no matter how exact the model is calibrated, there always exists discrepancy between model outcome and observed data (Chiang et al., 2007; Beven, 2006).

3.4.4 Natural Uncertainty

Natural uncertainty arises due to the randomness of natural processes (Beven, 2001). This uncertainty can be linked to data uncertainty, whereby the quality and type of data plays a significant role in determining the amount of uncertainty. For example, the spatial and temporal randomness of rainfall can somewhat be represented explicitly when using good rain gauge networks and radar rainfall data (Segond, 2006). In addition, scaling issues, spatial representativity and interpolation methods are typically represented within natural uncertainty (Heuvelink, 1998; Blöschl, 1999).

For this study, the meaning of "within uncertainty" is considered to be within +/-20 percent and was based on several factors. This range is based on AWA's extensive professional experience evaluating each of these factors below and how they relate to the PMP calculations:

- Multiple sources of uncertainty and varying ranges of uncertainty inherent in the PMP development process and inputs
    - Gauge/Observed Precipitation
        - Point measurement 5 to 15% percent for long-term series, and as high as 75% for individual storm events
    - Frequency Analysis
        - NOAA Atlas 14 Volume 1 24-hour 100-year error bounds for Arizona are approximately +/-18% (Bonin et al., 2011)
    - Climate Projections
        - Projection uncertainty for induvial regional model methods can be quite large 20 to >50% (Lehner et al., 2020)
    - Selection of the storm representative value used in the In-place Maximization Factor calculations
        - Range between 5 and 30%, with an average around 20%

4.0 RESULTS OF ANALYSIS

The modeled trends and estimated precipitation frequency results have a large variability that can be attributed to the uncertainty inherent with GCM and RCM projections. The different climate models used for the Chino/Tyrone region are subject to significant components of future climate uncertainty in climate models and the uncertainty is manifested by the range of climate futures indicated by the CMIP5 ensemble of projections (McSweeney and Jones, 2016; Masson-Delmotte et al., 2021).

The median of the five models project an increase in mean annual temperature and mean annual precipitation (Figure 13). Temperature, in regard to daily maximum (frequency based) and monthly averages show an increase by 2100 for both the RCP 4.5 and RCP 8.5 projections (Figure 14 and Figure 15). Numeric values representing the change in temperature are shown in Table 5 and Table 7 under application of results. Monthly climatologies for temperature and precipitation are shown in Figure 15 and Figure 16, numeric values representing the change in temperature and precipitation are shown in Table 5 and Table 8 under application of results.

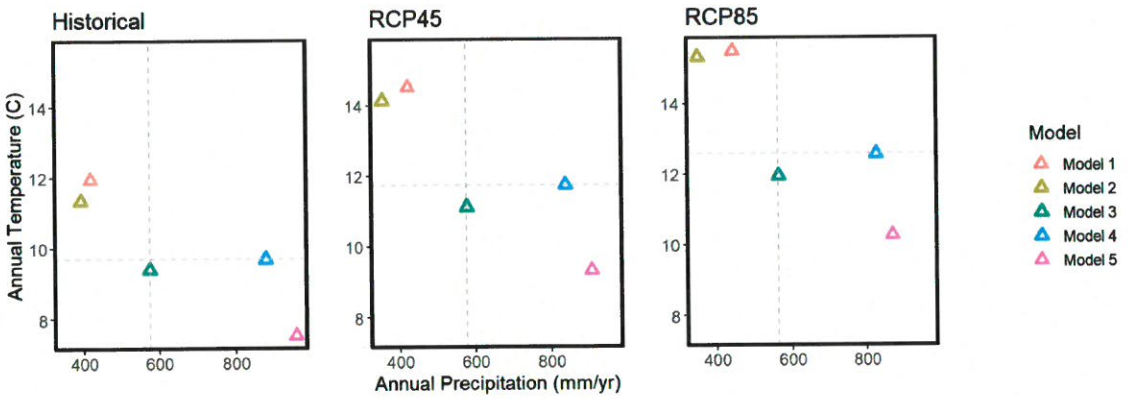

Figure 13: Comparison of mean annual temperature and mean annual precipitation for the three climate projection periods. The grey dashed lines represent the median value for annual average temperature and precipitation.

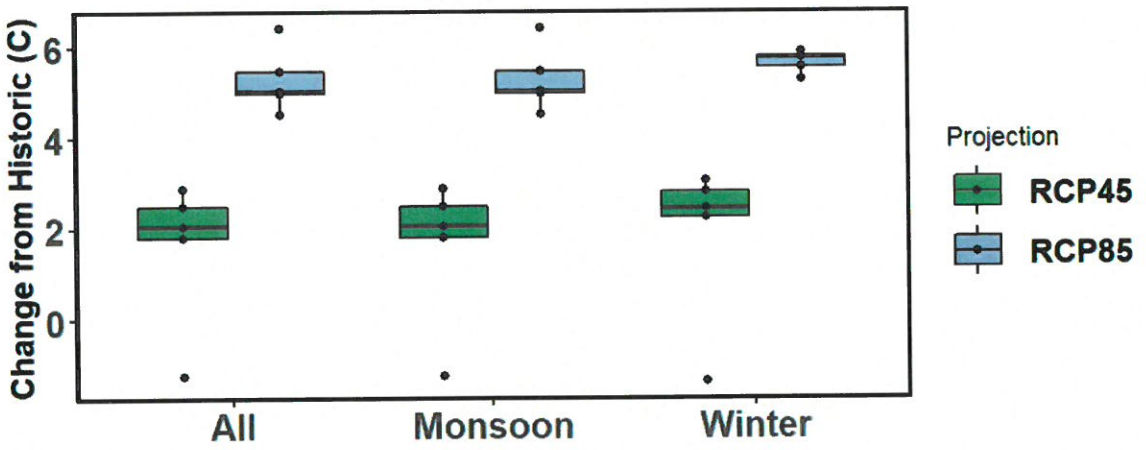

Figure 14: Change in daily maximum temperatures from current climate conditions. Results are based on annual maximum frequency analysis.

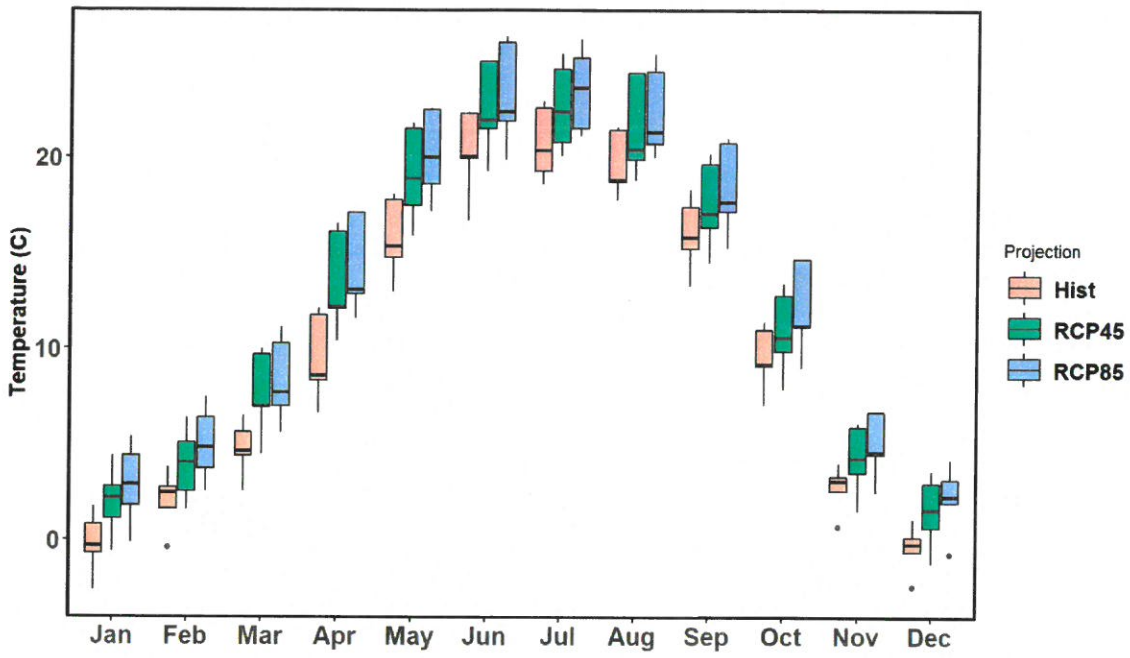

Figure 15: Monthly temperature normal compared to climate change temperature. Results are based on daily normal calculations.

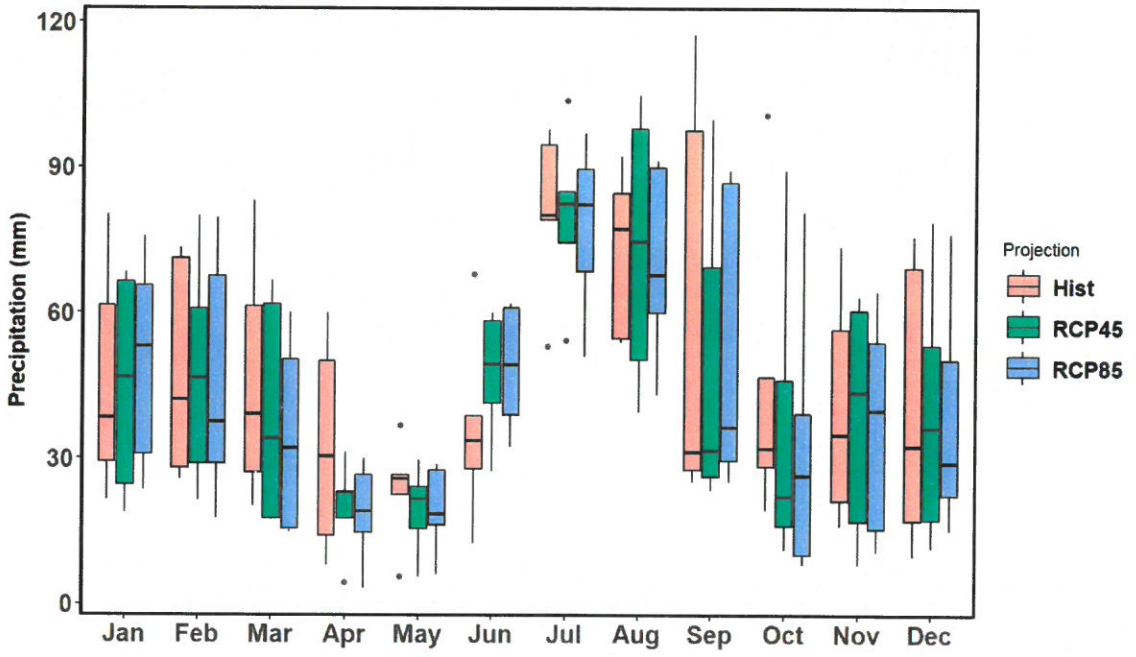

Figure 16: Monthly precipitation normal compared to climate change precipitation. Results are based on daily normal calculations.

Precipitation frequency analysis results are summarized for 1-day, 3-day, and annual durations split by All season, Summer/Monsoon season and Winter season (Figure 17). Results indicate a

broad range of change with the largest change for 1-day and 3-day durations, numeric values representing the change in precipitation are shown in Table 5.

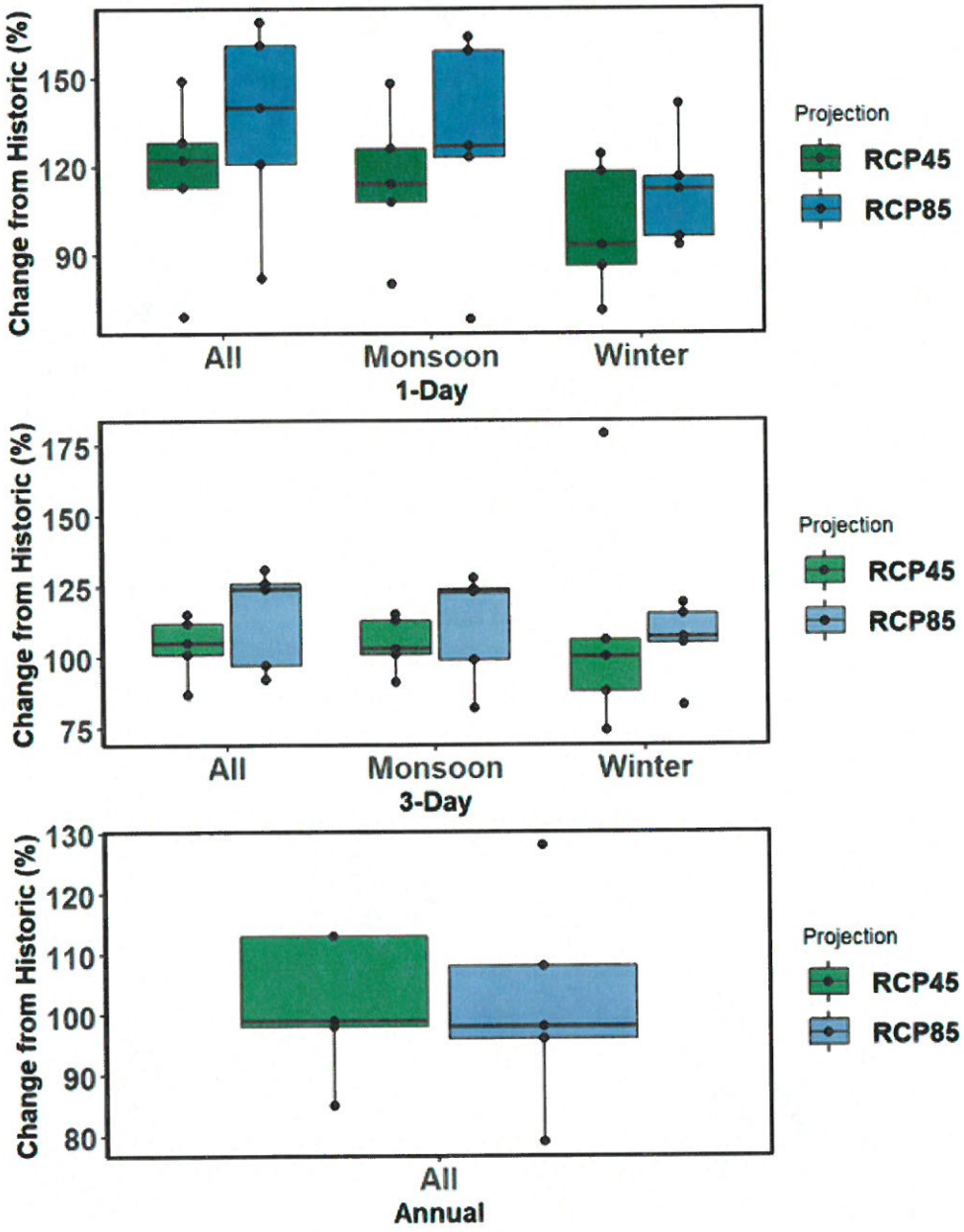

Figure 17: Change in maximum precipitation from current climate conditions for 1-day, 3-day, and annual durations. Results are based on annual maximum frequency analysis. Note, the AMS frequency approach shows a decrease in annual precipitation as compared to the mean annual climatology method which shows an increase.

Results indicate an increase in precipitation and temperature in the future. The range of uncertainty and potential future outcomes are captured in Figure 17. The most likely outcome regarding precipitation over the basin in the climate change projections is that the mean annual precipitation

will stay the same and short duration events (1-day and 3-day) will likely increase compared to the current climate. Importantly, the climate change projections show that individual extreme events that are utilized for PMP development will stay within the range of uncertainty currently inherent in the PMP depths.

This follows expected trends in the region under a warming climate scenario. In this case, more moisture would be available from an overall perspective, and would likely affect some of the precipitation processes, but this would likely be counteracted by other processes that are required to produce precipitation at various timescales and spatial extents (Kappel et al., 2020). This is reflected in Table 5 where the RCP4.5 emission scenario shows a decrease in annual precipitation and increase on 1- and 3-day values. This is likely a reflection of the variance in atmospheric processes that convert moisture in the atmosphere to rainfall on the ground and other factors not fully understood or quantified. These create both positive and negative feedbacks where atmospheric instability at the most extreme levels are lessened in a warming environment because the thermal contrast between airmass is lessened.

5.0 APPLICATION OF RESULTS

For hydrologic simulation and sensitivity, AWA recommends the ensemble median RCP 4.5 climate change adjustments and uncertainty values for temperature and precipitation (Table 5, Table 7, and Tale 8). These are based on an evaluation of rate of change from the current period through 2100 of each of the projections and taking a median of the outcomes. These values can be applied to a given period (i.e., 2050) by linearly adjusting the climate change factors. Table 6 illustrates how the recommended RCP 4.5 climate change adjustments can be scaled the linear from 2100 to 2050.

In regard to PMP changes, there is no clear evidence for appropriate scaling adjustments, for sensitivity it is recommended to apply the precipitation frequency results shown in Table 5 and Table 6. The climate model projections tended to underestimate the storm representative moisture used to maximize against the 100-year climatologies (Section 3.3.2), which resulted in the underestimation of the maximization factor where several of the ratios were capped at 1.50 (Kappel et al., 2020). This will skew the ratio analysis to larger changes. These analyses show that it is likely that the frequency of a PMP event may increase in the future, but the amount of rainfall produced in a given PMP would fall within the current depths. Therefore, if a given hydrologic design can safely pass the current PMP depths, then the design would be considered adequate to manage future PMP changes.

Table 5: Climate Change Projections from current climate (1950-2005) through 2100.

	RCP45				RCP85			
	Mean	**Median**	**Min**	**Max**	**Mean**	**Median**	**Min**	**Max**
Temperature 1-Day; C	**1.6**	**2.1**	-1.3	2.9	**5.3**	**5.0**	4.5	6.4
Temperature 1-Day Monsoon PF; C	**1.6**	**2.1**	-1.3	2.9	**5.3**	**5.0**	4.5	6.4
Temperature 1-Day Winter PF; C	**1.8**	**2.4**	-1.4	3.0	**5.6**	**5.8**	5.3	5.9
+Precipitation 1-Day PF; %	**16**	**22**	-31	49	**35**	**40**	-18	69
Precipitation 1-Day Monsoon PF; %	**15**	**14**	-20	48	**28**	**27**	-32	64
Precipitation 1-Day Winter PF; %	**-1**	**-7**	-29	24	**12**	**12**	-7	41
+Precipitation 3-Day PF; %	**4**	**5**	-13	15	**14**	**24**	-8	31
Precipitation 3-Day Monsoon PF; %	**5**	**3**	-9	15	**11**	**23**	-18	28
Precipitation 3-Day Winter PF; %	**9**	**0**	-26	79	**6**	7	-17	19
Precipitation Annual PF; %	**2**	**-1**	-15	13	**2**	**-2**	-21	28
PMP 1-Day, %	**No Change**				**Potential Increase**			
PMP 3-Day; %	**No Change**				**No Change**			

* Climate Change Projections from 2005 through 2100

\+ Note, RCP 8.5 represent the most extreme, unlikely climate projection scenarios

Table 6: Recommended RCP 4.5 climate change adjustments (%) for 1-day and 3-day precipitation scaled from 2100 to 2050

	2050	**2100**
1-Day Summer PF; %	7	14
1-Day Winter PF; %	-3	-7
3-Day Summer PF; %	2	3
3-Day Winter PF; %	0	0

Climate Change Projections from 2005 through 2100

Table 7: Monthly temperature (C) for current climate from 2005 through 2100.

	Historical		RCP45		RCP85		Mean Delta		Median Delta	
	Mean	Median	Mean	Median	Mean	Median	RCP45	RCP85	RCP45	RCP85
January	-0.2	-0.3	2.0	2.2	2.9	2.9	*2.2*	*3.1*	*2.5*	*3.2*
February	2.1	2.5	3.9	4.1	5.0	4.9	*1.9*	*2.9*	*1.6*	*2.4*
March	4.8	4.7	7.6	7.0	8.3	7.7	*2.9*	*3.6*	*2.4*	*3.1*
April	9.5	8.6	13.5	12.2	14.3	13.1	*4.0*	*4.9*	*3.6*	*4.5*
May	15.8	15.4	19.1	18.9	20.2	20.0	*3.3*	*4.4*	*3.6*	*4.7*
June	20.3	20.1	22.6	22.0	23.3	22.4	*2.3*	*3.0*	*1.9*	*2.4*
July	20.8	20.4	22.7	22.4	23.5	23.6	*1.9*	*2.8*	*2.1*	*3.3*
August	19.7	18.8	21.6	20.4	22.4	21.3	*1.9*	*2.7*	*1.6*	*2.5*
September	16.0	15.9	17.6	17.1	18.4	17.7	*1.5*	*2.4*	*1.2*	*1.8*
October	9.6	9.2	10.9	10.6	12.2	11.2	*1.4*	*2.6*	*1.4*	*2.0*
November	2.8	3.1	4.3	4.3	5.0	4.6	*1.5*	*2.2*	*1.2*	*1.5*
December	-0.4	-0.2	1.5	1.6	2.2	2.3	*1.9*	*2.6*	*1.8*	*2.5*

Table 8: Monthly precipitation (mm) for current climate from 2005 through 2100.

	Historical		RCP45		RCP85		Mean Delta		Median Delta	
	Mean	Median	Mean	Median	Mean	Median	RCP45	RCP85	RCP45	RCP85
January	46.1	38.3	44.9	46.6	49.7	53.1	*-1.2*	*3.6*	*8.4*	*14.9*
February	48.0	42.1	47.5	46.5	46.3	37.6	*-0.6*	*-1.8*	*4.5*	*-4.5*
March	46.1	39.2	39.5	34.1	34.6	32.1	*-6.7*	*-11.6*	*-5.1*	*-7.1*
April	32.5	30.4	19.9	23.0	18.7	19.0	*-12.6*	*-13.8*	*-7.4*	*-11.4*
May	23.4	25.8	19.3	21.5	19.4	18.5	*-4.2*	*-4.0*	*-4.3*	*-7.3*
June	36.1	33.6	47.3	49.4	48.7	49.3	*11.2*	*12.6*	*15.9*	*15.8*
July	80.9	80.1	79.9	82.4	77.7	82.3	*-1.0*	*-3.2*	*2.4*	*2.3*
August	72.6	77.3	73.5	74.6	70.5	67.8	*0.9*	*-2.1*	*-2.7*	*-9.5*
September	59.8	31.3	50.1	31.6	53.4	36.4	*-9.7*	*-6.4*	*0.3*	*5.1*
October	45.4	32.0	37.0	22.1	33.0	26.4	*-8.4*	*-12.5*	*-9.9*	*-5.6*
November	40.5	34.9	38.5	43.6	36.9	39.9	*-2.0*	*-3.7*	*8.7*	*5.0*
December	40.9	32.5	39.5	36.2	38.7	29.1	*-1.4*	*-2.2*	*3.7*	*-3.4*

6.0 CONCLUSIONS

The Chino/Tyrone climate change analysis investigated CMIP5 projections. The projections were evaluated using several statistical methodologies to test for trends in temperature and precipitation, changes in precipitation frequency, and changes in monthly climatologies. The results have large variability that can be attributed to the uncertainties and limitations inherent in climate model projections and the physical representation of meteorological parameters such as precipitation.

The trend and frequency analysis methods provide a robust dataset to test changes in precipitation and temperature. The moisture maximization method discussed in Section 3.3 is an investigation into one of the most important parameters related to PMP calculation, the amount of moisture available in the atmosphere. This is a simplification of methods used to estimate a storm-based PMP. The main differences are that a complete PMP study develops storms specific reconstructions and adjustments including identification of the storm representative dew point values for observed PMP type storms and application of storm transposition limits (Kappel et al., 2018). Therefore, more confidence is given to the trend and precipitation frequency results as compared to the moisture maximization ratio analysis. The five climate models average relative change in dew point are about 1.4 °C (~11%) warmer for RCP45 and 2.3 °C (~17%) warmer for RCP85, with negligible change in the summer (May – October) dew point climatologies and larger increase in moisture during the early winter to spring period (Figure 18). For RCP45, Figure 18 illustrates the potential for the storm moisture maximization ratio to increase but these results are typically less than the +/-20% uncertainty (except for February). Importantly, the smallest increase occurs during the summer North American Monsoon season. The projections demonstrate that no change to PMP depths is evident because these changes are within the range of uncertainty already captured in the PMP depths.

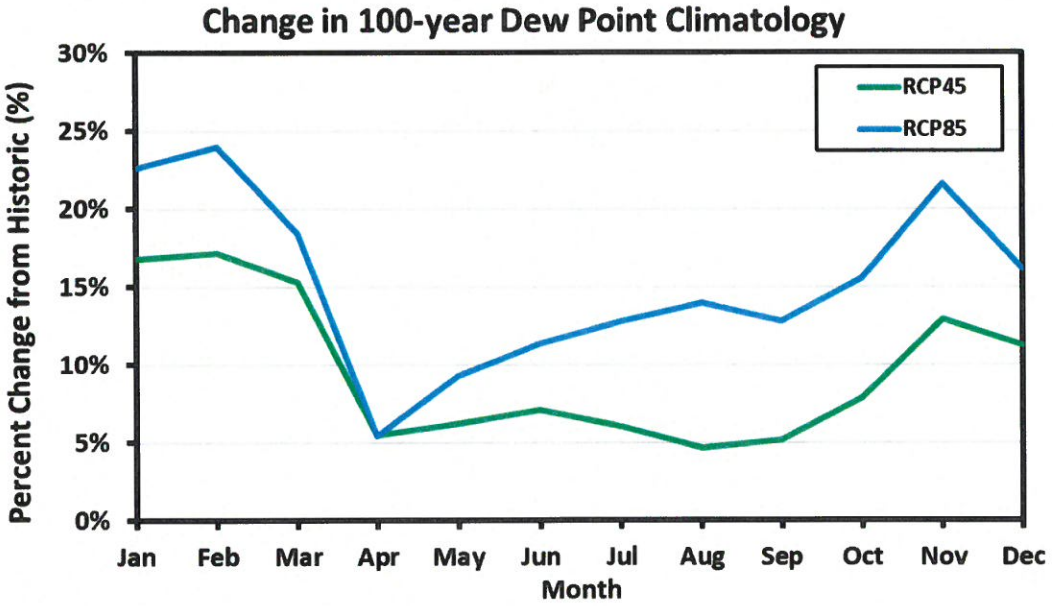

Figure 18: Change in 100-year dew point climatologies from the historic period. Dew point climatologies are used to account for changes in moisture under different climate scenarios.

The climate change analysis completed for the Chino/Tyrone Mine was based on five CMIP5 climate model projections and three climate scenarios (historic, RCP 4.5, and RCP 8.5). A summary of the key conclusions from this study are listed below.

TREND ANALYSIS

- Surface stations show no historic change/trend in precipitation and temperature
- Projections show increase in temperature and dew point temperature

- RCP 4.5 precipitation - No trend
- RCP 8.5 precipitation - 1-day and 3-day no trend, annual increase/decrease trend

FREQUENCY ANALYSIS

- **1-day** – the median RCP 4.5 results are within the +/-20% uncertainty which provide more confidence for no change in precipitation magnitude by 2100. RCP 8.5 winter results are within the +/-20% uncertainty which provide more confidence for no change in precipitation magnitude by 2100 while the RCP 8.5 monsoon median value is larger than the +/-20% uncertainty which provide more confidence for an increase in precipitation magnitude by 2100
  - largest change in both summer monsoon seasons
- **3-day** – the median RCP 4.5 results are within the +/-20% uncertainty which provide more confidence for no change in precipitation magnitude by 2100. RCP 8.5 winter results are within the +/-20% uncertainty which provide more confidence for no change in precipitation magnitude by 2100 while the RCP 8.5 monsoon median value is larger than the +/-20% uncertainty which provide more confidence for an increase in precipitation magnitude by 2100
  - largest change in summer monsoon season
- **Annual** – no change of precipitation magnitude by 2100 and increase temperature by 2100

MOISTURE MAXIMIZATION ANALYSIS

- Projections do not show an increase or decrease of the moisture scaling factor that is beyond the range of uncertainty already in the PMP development
- Median dew point climatologies are 1.8 °C (~10%) warmer for RCP 4.5 and 2.9 °C (~15%) warmer for RCP 8.5
- One recommendation is to apply the precipitation frequency results for sensitivity. This may result in a higher probability of a PMP event occurring in any given year, but the PMP depths are not expected to increase

CLIMATOLOGY

- **Monthly Climatology** – Some months show a slight increase, and some months show a decrease in precipitation. All months show an increase in temperature by 2100
- **Annual Climatology** – Some models show a slight increase, and some models show a decrease in annual precipitation. All months show an increase in annual temperature by 2100

7.0 REFERENCES

Beven, K.J., 2001. *Rainfall-runoff modelling: The Primer*. John Willey and Sons, Chichester, UK. pp 360.

Beven, K.J., 2006. A manifesto for the equifinality thesis. *Journal of Hydrology,* 320, 18-36.

Blösch, G., 1999. Scaling Issues in Snow Hydrology. *Hydrological Processes*, 13, 2149- 2175.

Bonnin, G.M., Todd, D., Lin, B., Parzybok, T., Yekta, M., and D. Riley, 2006: Precipitation-Frequency Atlas of the United States, NOAA Atlas 14, Volumes 1 and 2, NOAA, National Weather Service, Silver Spring, Maryland. http://hdsc.nws.noaa.gov/hdsc/pfds/

Chaing, S., Y. Tachikawa, and K. Takara, 2007. Hydrological model performance comparison through uncertainty recognition and quantification. *Hydrological Processes*, 21, 1179-1195.

Hansen, E.M., Fenn, D.D., Schreiner, L.C., Stodt, R.W., and J.F., Miller, 1988: Probable Maximum Precipitation Estimates, United States between the Continental Divide and the 103rd Meridian, *Hydrometeorological Report Number 55A*, National weather Service, National Oceanic and Atmospheric Association, U.S. Dept of Commerce, Silver Spring, MD, 242 pp.

Hausfather, Zeke; Peters, Glen P., 2020. "Emissions – the 'business as usual' story is misleading". Nature. 577 (618–620). doi:10.1038/d41586-020-00177-3. Retrieved 2022-03-28.

Heuvelink, G., 1998. *Error Propagation in Environmental Modelling with GIS*. CRC Press, 150 pp.

Hipel, K.W. and McLeod, A.I., (2005). Time Series Modelling of Water Resources and Environmental Systems. Electronic reprint of our book originally published in 1994. http://www.stats. uwo.ca/faculty/aim/1994Book/.

Hosking, J.R.M, 2015a. L-moments. R package, version 2.5. URL: http://CRAN.R-project.org/package=lmom.

Hosking, J.R.M, 2015b. Regional frequency analysis using L-moments. R package, version 3.0-1. URL: http://CRAN.R-project.org/package=lmomRFA.

Hosking, J.R.M. and J.R. Wallis, 1997, "Regional Frequency Analysis, An Approach Based on L-Moments," Cambridge University Press, 224 pp.

IPCC, 2017. Intergovernmental Panel on Climate Change (IPCC) Fifth Assessment Report (AR5) Observed Climate Change Impacts Database, Version 2.01. Palisades, NY: NASA

Socioeconomic Data and Applications Center (SEDAC). https://doi.org/10.7927/H4FT8J0X.

IPCC, 2021: Climate Change 2021: The Physical Science Basis. Contribution of Working Group I to the Sixth Assessment Report of the Intergovernmental Panel on Climate Change [Masson-Delmotte, V., P. Zhai, A. Pirani, S.L. Connors, C. Péan, S. Berger, N. Caud, Y. Chen, L. Goldfarb, M.I. Gomis, M. Huang, K. Leitzell, E. Lonnoy, J.B.R. Matthews, T.K. Maycock, T. Waterfield, O. Yelekçi, R. Yu, and B. Zhou (eds.)]. Cambridge University Press. In Press.

Kampf, S.K., et al., 2020. The case for an open water balance: Re-envisioning network design and data analysis for a complex, uncertain world. *Water Resources Research*, 56(6), e2019WR026699. https://doi.org/10.1029/2019WR026699

Kappel, W.D., Hultstrand, D.M., Muhlestein, G.A., Steinhilber, K., McGlone, D., Parzybok, T.W, and E.M. Tomlinson, December 2014: Statewide Probable Maximum Precipitation (PMP) Study for Wyoming.

Kappel, W.D., Hultstrand, D.M., Muhlestein, G.A., Steinhilber, K., McGlone, D., Rodel, J., and B. Lawrence, November 2018: Regional Probable Maximum Precipitation for the States of Colorado and New Mexico. Prepared for the Colorado Division of Water Resources and the New Mexico State Engineers Office.

Kappel, W.D., Hultstrand, D.M., Steinhilber, K., and J.T. Rodel, 2020: Climate Change and PMP: Are These Storms Changing? *Journal of Dam Safety*, Vol. 17, No. 3 (in press).

Koren, V.I., B.D. Finnerty, J.C. Schaake, M.B. Smith, D.J. Seo, and Q. Duan, 1999. Scale dependencies of hydrologic models to spatial variability of precipitation. *Journal of Hydrology*, 217, 285-302.

Lehner, F., Deser, C., Maher, N., Marotzke, J., Fischer, E. M., Brunner, L., Knutti, R., and Hawkins, E., 2020. Partitioning climate projection uncertainty with multiple large ensembles and CMIP5/6, Earth Syst. Dynam., 11, 491–508, https://doi.org/10.5194/esd-11-491-2020

Mann, H.B. (1945), Nonparametric tests against trend, Econometric, 13, 245-259.

Mantovan, P., and E. Tondini, 2006. Hydrological forecasting uncertainty assessment: Incoherences of the GLUE methodology. *Journal of Hydrology*, 330(1-2), 368-381.

Masson-Delmotte, Valérie; Zhai, Panmao; Pirani, Anna; Connors, Sarah L.; Péan, Clotilde; Berger, Sophie; Caud, Nada; Chen, Yang; Goldfarb, Leah; Gomis, Melissa I.; Huang, Mengtian; Leitzell, Katherine; Lonnoy, Elisabeth; Matthews, J. B. Robin; Maycock, Tom K.; Waterfield, Tim; Yelekçi, Ozge; Yu, Rong; Zhou, Baiquan, eds., 2021. "Summary for Policymakers". Climate Change 2021: The Physical Science Basis. Contribution of Working Group I to the Sixth Assessment Report of the Intergovernmental Panel on Climate Change (PDF). IPCC / Cambridge University Press.

McLeod, A.I., 2015. Kendall: Kendall rank correlation and Mann-Kendall trend test. R package, version 2.2. URL: https://cran.r-project.org/web/packages/Kendall/index.html.

McSweeney, C.F., Jones, R.G., 2016. How representative is the spread of climate projections from the 5 CMIP5 GCMs used in ISI-MIP? Climate Services vol 1, 24–29. https://doi.org/10.1016/j.cliser.2016.02.001

Perica, S., Pavlovic, S., Laurent, M.S., Trypaluk, D. Unruh, Martin, D., and O. Wilhite, 2015: *NOAA Atlas 14 Volume 10 version 2, Precipitation-Frequency Atlas of the United States, Northeastern States,* NOAA, National Weather Service, Silver Spring, MD.

Pokorny S. et al., 2021. Cumulative Effects of Uncertainty on Simulated Streamflow in a Hydrologic Modeling Environment. Elementa: Science of the Anthropocene 9(1) 431. https://doi.org/10.1525/elementa.431

Rousseau, A.N., I.M. Klein, D. Freudiger, P. Gagnon, A. Frigon, C. Ratté-Fortin, 2014: Development of a methodology to evaluate probable maximum precipitation (PMP) under changing climate conditions: application to southern Quebec, Canada, *J. Hydrol.*, 519 (2014), pp. 3094-3109.

Scharffenberg, B., Bartles, M., Brauer, T., Fleming, M., Karlovits, G. 2018. Hydrologic Modeling System HEC-HMS – User's Manual, Version 4.3. U.S. Army Corps of Engineers, Institute for Water Resources, Hydrologic Engineering Center (CEIWR-HEC), Davis, CA, USA.

Segond, M.L., C. Onof, and H.S. Wheater, 2006. Spatial-temporal disaggregation of daily rainfall from a generalized linear model. *Journal of Hydrology*, 331, 674-689.

Thrasher, B., Wang, W., Michaelis, A. Nemani, R., 2021. NEX-GDDP-CMIP6. NASA Center for Climate Simulation, doi:10.7917/OFSG3345.

Thrasher, B., Wang, W., Michaelis, A., Melton, F., Lee, T., Nemani, R., 2022. NASA Global Daily Downscaled Projections, CMIP6. Nature Scientific Data (in review)

US Weather Bureau, 1951, Tables of Precipitable Water and Other Factors for a Saturated Pseudo-adiabatic Atmosphere, *Technical Paper Number 14*, US. Department of Commerce, Washington, DC, 66 pp.

Wagener, T., H.S. Wheather, and H.V. Gupta, 2004. *Rainfall-runoff modelling in gauged and ungauged catchments*. Imperial College Press, London pp 306.

World Meteorological Organization, 2009: Manual for Estimation of Probable Maximum Precipitation, No. 1045, WMO, Geneva, 259 pp